Progress In Electromagnetics Research, PIER 99, 453–463, 2009

ANALYSIS OF FINITE PERIODIC DIELECTRIC GRATINGS BY THE FINITE-DIFFERENCE FREQUENCY-DOMAIN METHOD WITH THE SUB-ENTIRE-DOMAIN BASIS FUNCTIONS AND WAVELETS

G. Zheng, B.-Z. Wang, H. Li, X.-F. Liu, and S. Ding

Institute of Applied Physics
University of Electronic Science and Technology of China
Chengdu 610054, China

Abstract—In this paper, the finite-difference frequency-domain (FDFD) method, boundary integral equation (BIE) method and sub-entire-domain (SED) basis functions are combined to analyze scatterings from finite periodic dielectric gratings. The wavelet method is used to reduce the number of inner product operations in calculating the mutual-impedance elements between the SED basis functions. In the numerical examples, the RCS curves obtained by the method in this paper are in good agreement with those obtained by the classical full-domain FDFD method, but the computational times are largely reduced and no large matrix equation needs to be stored and solved in the former.

1. INTRODUCTION

The finite-difference frequency-domain (FDFD) method [1, 2] and the method of moments (MoM) [3, 4] are very powerful numerical methods and widely applied to many electromagnetic problems. The MoM is efficient because only scatterers need to be discretized. The FDFD method is flexible when a complicated structure is analyzed, and the final matrix equation is a sparse one. The two methods were combined together [5]. Difference equations are set up inside the computational domain, and a boundary integral equation (BIE) is used as a global absorbing boundary condition to truncate the computational domain. Compared with local absorbing boundary conditions, this global absorbing boundary condition can be close to the object and should be more globally accurate. But because the BIE

Corresponding author: G. Zheng (zhenggang@uestc.edu.cn).

method is used on the boundary, the number of non-zero elements in the final matrix equation of the FDFD-BIE method rises rapidly, when a large object, such as a large array, is analyzed. The sub-entire-domain (SED) basis functions for the MoM were proposed [6, 7] and used to analyze large finite periodic metal arrays [8–10]. In this efficient technique, the periodic property is considered, and the mutual coupling is approximately treated, so the number of unknowns can be dramatically reduced. Accordingly, the efficiency is improved, and the cost of storage is reduced.

In this paper, the advantages of the FDFD method's flexibility and the MoM's high efficiency are taken, and finite periodic dielectric gratings are analyzed by combining the FDFD method, the BIE method and the SED basis functions. As shown in Figure 1, three sub-domains which include an element and its nearby elements respectively are discretized with Yee's cells [11], and the classical FDFD equations are set up at the nodes of Yee's cells. On the boundaries of them, a boundary integral equation is set up, and rectangular pulse functions are used as sub-domain basis functions to represent the distributions of the tangential field and its normal derivative on the boundaries of the three sub-domains. The SED basis functions are extracted

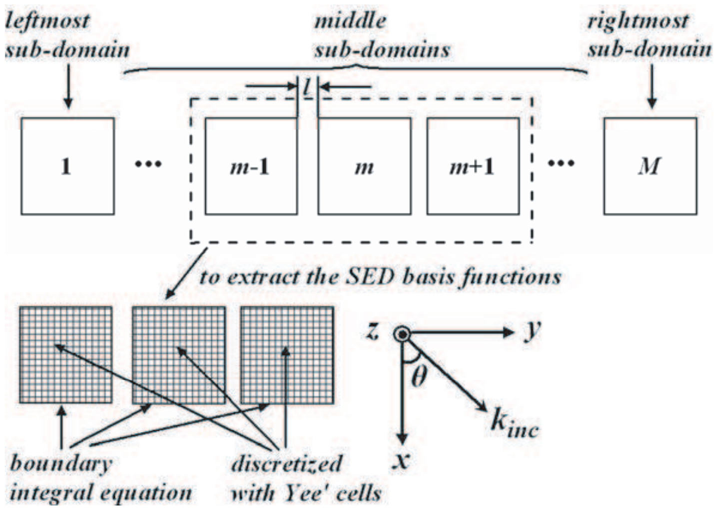

Figure 1. The M elements are included in the M sub-domains, whose boundaries are close to the elements. Three adjacent sub-domains are separated from the M sub-domains in order to extract the SED basis functions for the whole grating. They are discretized with Yee's cells, and a boundary integral equation is set up on their boundaries.

through the above process and adopted as the sub-domain basis functions for the boundary of the whole dielectric grating. After the Galerkin's procedure, the expansion coefficients of the SED basis functions can be decided, and accordingly the distributions of the tangential field and its normal derivative on the boundary of the whole dielectric grating are obtained. Then the radar cross section (RCS) of the dielectric grating can be computed through near-field to far-field (NF-FF) transformation. Additionally, before the mutual-impedance elements between the SED basis functions are calculated, the SED basis functions are modified through the wavelet method. Their expressions expanded by uniform rectangular pulse functions are changed to be expanded by non-uniform rectangular pulse functions with difference sizes, so the number of rectangular pulse functions which are used to represent the SED basis functions is reduced, and accordingly the number of inner product operations in calculating the mutual-impedance elements is reduced. The whole above process is described in Section 2 in detail. The numerical results of the method in this paper are given and compared with those of the classical full-domain FDFD method in Section 3. And some conclusions are following in Section 4.

2. FORMULATION

2.1. The FDFD-BIE Method

As shown in Figure 1, the grating is uniform in the z-direction, and the M elements are included in the M corresponding sub-domains.

Here the case of TE wave is considered, and the case of TM wave can be handled in a similar way. When the grating is illuminated by TE wave, the following integral equation should be satisfied on the boundary.

$$H_z^{inc}(\boldsymbol{\rho}) = H_z^t(\boldsymbol{\rho}) - \oint_\Gamma H_z^t(\boldsymbol{\rho}') \frac{\partial G(\boldsymbol{\rho}, \boldsymbol{\rho}')}{\partial \mathbf{n}'} d\Gamma' + \oint_\Gamma \frac{\partial H_z^t(\boldsymbol{\rho}')}{\partial \mathbf{n}'} G(\boldsymbol{\rho}, \boldsymbol{\rho}') d\Gamma' \quad \boldsymbol{\rho} \text{ on } \Gamma \quad (1)$$

where H_z^t and H_z^{inc} are the z-components of the total magnetic field and the incident magnetic field respectively. $G(\boldsymbol{\rho}, \boldsymbol{\rho}')$ is the two-dimensional Green's function in free space. $\boldsymbol{\rho}$ and $\boldsymbol{\rho}'$ are position vectors. $\mathbf{n}$ is normal to the boundary and outward of the sub-domains, and $\frac{\partial}{\partial \mathbf{n}'}$ is $\mathbf{n}$-directional derivative with regard to $\boldsymbol{\rho}'$. Three adjacent sub-domains are separated from the M sub-domains to extract the SED basis functions, which are based on the basic idea that the mutual coupling of a sub-domain with its neighbor sub-domains is dominant.

In case of strong mutual coupling, more than three sub-domains should be used to extract the sub-entire-domain basis functions so that the mutual coupling effect of a sub-domain with more its nearby sub-domains can be taken into account. These sub-domains are discretized with Yee's cells, and the classical FDFD equations are set up at the nodes of Yee's cells. Rectangular pulse function $U_n(\boldsymbol{\rho})$ is adopted as sub-domain basis function to represent H_z^t and $\frac{\partial H_z^t}{\partial \mathbf{n}}$ as follows on the boundary Γ which is composed of the boundaries of the three sub-domains as shown in Figure 1.

$$H_z^t(\boldsymbol{\rho}) = \sum_{n=1}^{3N} a_n U_n(\boldsymbol{\rho}), \quad \frac{\partial H_z^t(\boldsymbol{\rho})}{\partial n} = \sum_{n=1}^{3N} b_n U_n(\boldsymbol{\rho}) \tag{2}$$

where N is the number of the sub-domain basis functions on the boundary of a sub-domain. After the above expressions are substituted into (1), (3) is gotten by the Galerkin's procedure.

$$\begin{bmatrix} Z_{1,1}^{(1)} & Z_{1,2}^{(1)} & \cdots & Z_{1,3N}^{(1)} \\ Z_{2,1}^{(1)} & Z_{2,2}^{(1)} & \cdots & Z_{2,3N}^{(1)} \\ \vdots & \vdots & \ddots & \vdots \\ Z_{3N,1}^{(1)} & Z_{3N,2}^{(1)} & \cdots & Z_{3N,3N}^{(1)} \end{bmatrix} \begin{bmatrix} a_1 \\ a_2 \\ \vdots \\ a_{3N} \end{bmatrix} + \begin{bmatrix} Z_{1,1}^{(2)} & Z_{1,2}^{(2)} & \cdots & Z_{1,3N}^{(2)} \\ Z_{2,1}^{(2)} & Z_{2,2}^{(2)} & \cdots & Z_{2,3N}^{(2)} \\ \vdots & \vdots & \ddots & \vdots \\ Z_{3N,1}^{(2)} & Z_{3N,2}^{(2)} & \cdots & Z_{3N,3N}^{(2)} \end{bmatrix} \begin{bmatrix} b_1 \\ b_2 \\ \vdots \\ b_{3N} \end{bmatrix} = \begin{bmatrix} g_1 \\ g_2 \\ \vdots \\ g_{3N} \end{bmatrix} \tag{3}$$

where $Z_{m,n}^{(1)} = \langle U_m, L_1(U_n) \rangle$, $Z_{m,n}^{(2)} = \langle U_m, L_2(U_n) \rangle$, $g_m = \left\langle U_m, H_z^{inc} \right\rangle$, $L_1(U) = U - \oint_\Gamma U \frac{\partial G}{\partial n'} d\Gamma'$ and $L_2(U) = \oint_\Gamma U G d\Gamma'$.

Additionally, there exist the following two relationships between the unknown expansion coefficients in (2) and the unknown total field values at the nodes of Yee's cells.

Relationship 1: $[a_1, a_2, \ldots, a_{3N}]$ equal to the average values of H_z^t on the two outmost layers of the H_z^t nodes of Yee's cells.

Relationship 2: $[b_1, b_2, \ldots, b_{3N}]$ can be expressed by the tangential total electric field values on the outmost layer of the corresponding nodes of Yee's cells.

After combining (3), the two relationships and the classical FDFD equations inside the three sub-domains, a matrix equation can be obtained as follows, which is a Schur complement system and can be solved in a parallel manner [12].

$$\begin{bmatrix} A_{L,L} & 0 & 0 & 0 & B_{L,a} \\ 0 & A_{M,M} & 0 & 0 & B_{M,a} \\ 0 & 0 & A_{R,R} & 0 & B_{R,a} \\ B_{b,L} & B_{b,M} & B_{b,R} & B_{b,b} & 0 \\ 0 & 0 & 0 & B_{a,b} & B_{a,a} \end{bmatrix} \begin{bmatrix} \phi_L \\ \phi_M \\ \phi_R \\ b \\ a \end{bmatrix} = \begin{bmatrix} 0 \\ 0 \\ 0 \\ 0 \\ g \end{bmatrix} \tag{4}$$

where ϕ_L, ϕ_M and ϕ_R are column vectors and represent the corresponding unknown total field values at all nodes of the Yee's cells in the left, middle and right sub-domains respectively. $a = [\tilde{a}_L, \tilde{a}_M, \tilde{a}_R]^T$ and $b = [\tilde{b}_L, \tilde{b}_M, \tilde{b}_R]^T$ whose components are the unknown expansion coefficients on the boundaries of the three sub-domains respectively. And $B_{a,a}a + B_{a,b}b = g$ is (3).

From (4), the column vectors a and b, that is, the distributions of H_z^t and its normal derivative $\frac{\partial H_z^t}{\partial \mathbf{n}}$ on the boundaries of the three sub-domains can be decided. It should be noted that the problem of three sub-domains only needs to be solved once to extract the SED basis functions for the whole grating. As for resonance cases of the boundary integral equation, a simple way could be used [13].

2.2. The SED Basis Function

Here, the physical interpretation of a SED basis function is that it is the distributions of H_z^t and its normal derivative $\frac{\partial H_z^t}{\partial \mathbf{n}}$ on the boundary of a sub-domain when only this sub-domain and its nearby sub-domains are illuminated and other sub-domains are ignored. For a grating, three kinds of the SED basis functions need to be considered which are corresponding to the leftmost sub-domain, the rightmost sub-domain and the middle sub-domains respectively, and the coefficients in the rectangular pulse function expansions of the three kinds of the SED basis functions are the elements of the column vectors $\tilde{a}_L$, $\tilde{b}_L$, the column vectors $\tilde{a}_R$, $\tilde{b}_R$, and the column vectors $\tilde{a}_M$, $\tilde{b}_M$ respectively, which have been gotten from (4). The rectangular pulse function expansions of the three kinds of the SED basis functions can be uniformly expressed as

$$U_m^{SED}(\boldsymbol{\rho}) = \sum_{n=1}^{N} \tilde{a}_{l_m,n} U_{m,n}(\boldsymbol{\rho}), \quad V_m^{SED}(\boldsymbol{\rho}) = \sum_{n=1}^{N} \tilde{b}_{l_m,n} U_{m,n}(\boldsymbol{\rho}) \tag{5}$$

where the subscript l_m represents 'L', 'R' or 'M' for the leftmost sub-domain, the rightmost sub-domain or the middle sub-domains respectively, and depends on m. These SED basis functions can be used as sub-domain basis functions to represent the distributions of H_z^t

and its normal derivative $\frac{\partial H_z^t}{\partial \mathbf{n}}$ on the boundary Γ of the whole grating (where $\Gamma = \Gamma_1 \cup \Gamma_2 \cup \ldots \cup \Gamma_M$, Γ_m is the boundary of Sub-domain m) as

$$\begin{bmatrix} H_z^t(\boldsymbol{\rho}) \\ \frac{\partial H_z^t(\boldsymbol{\rho})}{\partial n} \end{bmatrix} = \sum_{m=1}^{M} a'_m \begin{bmatrix} U_m^{SED}(\boldsymbol{\rho}) \\ V_m^{SED}(\boldsymbol{\rho}) \end{bmatrix} \tag{6}$$

After substituting (6) into (1), (7) can be obtained by testing (1) with functions $(V_1^{SED}, V_2^{SED}, \ldots, V_M^{SED})$.

$$\begin{bmatrix} Z'_{1,1} & Z'_{1,2} & \cdots & Z'_{1,M} \\ Z'_{2,1} & Z'_{2,2} & \cdots & Z'_{2,M} \\ \vdots & \vdots & \ddots & \vdots \\ Z'_{M,1} & Z'_{M,2} & \cdots & Z'_{M,M} \end{bmatrix} \begin{bmatrix} a'_1 \\ a'_2 \\ \vdots \\ a'_M \end{bmatrix} = \begin{bmatrix} g'_1 \\ g'_2 \\ \vdots \\ g'_M \end{bmatrix} \tag{7}$$

where $Z'_{m,n} = \langle V_m^{SED}, L_1(U_n^{SED}) + L_2(V_n^{SED})\rangle$ and $g'_m = \langle V_m^{SED}, H_z^{inc}\rangle$. When the expansion coefficients of the SED basis functions are decided from (7), the distributions of H_z^t and its normal derivative $\frac{\partial H_z^t}{\partial \mathbf{n}}$ on the boundary of the whole grating can be gotten by substituting these expansion coefficients into (6). Then the RCS of the grating can be obtained through NF-FF transformation.

2.3. Modify the SED Basis Functions with Haar Wavelets

The mutual-impedance element $Z'_{m,n}$ in (7) can be further expressed as

$$\begin{aligned} Z'_{m,n} = & \sum_{n_1=1}^{N} \sum_{n_2=1}^{N} \tilde{b}_{l_m,n_1} \tilde{a}_{l_n,n_2} \left\langle U_{m,n_1}, L_1\left(U_{n,n_2}\right)\right\rangle \\ & + \sum_{n_1=1}^{N} \sum_{n_2=1}^{N} \tilde{b}_{l_m,n_1} \tilde{b}_{l_n,n_2} \left\langle U_{m,n_1}, L_2\left(U_{n,n_2}\right)\right\rangle \end{aligned} \tag{8}$$

From (8), it can be seen that the computation of $Z'_{m,n}$ is very time-consuming, as it needs $2N^2$ inner product operations. The number of inner product operations can be reduced through reducing the number of rectangular pulse functions in (5). Rectangular pulse functions are Haar scaling functions, so through a process which is similar to filter noise, the expressions of the SED basis functions expanded by uniform rectangular pulse functions can be modified to be expanded by non-uniform rectangular pulse functions with different sizes. Firstly, the coefficients $(\tilde{a}_{M,n}, \tilde{b}_{M,n})$ in the expressions of the kind of the SED basis functions for the middle sub-domains are treated as follows. They are decomposed with Haar wavelets. $\alpha_{k,n}$ and $\beta_{k,n}$ denote coefficients of scaling functions and wavelet functions respectively where k is the index of the level and n is the index of the coefficient within each level. When $|\beta_{k,n}/\alpha_{k,n}|$ is smaller than a threshold value, $\beta_{k,n}$ is set to be zero. If the coefficients of two adjacent wavelet functions in the same level are zero, the coefficients of the two corresponding scaling functions are further decomposed. After decomposing, the multi-resolution wavelet coefficients are reconstructed, and then the adjacent scaling functions are combined, if the coefficients of them are the same. Now the coefficients in the non-uniform rectangular pulse function expansions of the kind of the SED basis functions for the middle sub-domains are gotten, and the expansions for Sub-domain m are

$$U_m^{SED}(\boldsymbol{\rho}) = \sum_{n=1}^{N^U} \tilde{a}'_{M,n} U_{m,n}^U(\boldsymbol{\rho}), \quad V_m^{SED}(\boldsymbol{\rho}) = \sum_{n=1}^{N^V} \tilde{b}'_{M,n} U_{m,n}^V(\boldsymbol{\rho}) \tag{9}$$

where $U_{m,n}^U$ and $U_{m,n}^V$ are non-uniform rectangular pulse functions. And the relationship between the coefficients $\tilde{a}'_{M,n}$, $\tilde{b}'_{M,n}$ and the coefficients $\tilde{a}_{M,n}$, $\tilde{b}_{M,n}$ can be expressed as

$$\tilde{a}'_M = A\tilde{a}_M, \quad \tilde{b}'_M = B\tilde{b}_M \tag{10}$$

where $\tilde{a}'_M = [\tilde{a}'_{M,1}, \ldots, \tilde{a}'_{M,N^U}]^T$, $\tilde{b}'_M = [\tilde{b}'_{M,1}, \ldots, \tilde{b}'_{M,N^V}]^T$, $\tilde{a}_M = [\tilde{a}_{M,1}, \ldots, \tilde{a}_{M,N}]^T$ and $\tilde{b}_M = [\tilde{b}_{M,1}, \ldots, \tilde{b}_{M,N}]^T$. The matrices A and B are decided by the above process of decomposing, reconstructing and combining. Now only $N^V\left(N^U + N^V\right)$ inner product operations are needed for calculating a mutual-impedance element, and N^U and N^V are smaller than N, so the efficiency is improved.

For a large grating the contribution from the leftmost element and the rightmost element is a small part of the contribution from the whole grating. So the coefficients in the expressions of the kinds of the SED basis functions for the leftmost sub-domain and the rightmost sub-domain can be simply treated as

$$\tilde{a}'_L = A\,\tilde{a}_L, \quad \tilde{b}'_L = B\,\tilde{b}_L \tag{11}$$

$$\tilde{a}'_R = A\,\tilde{a}_R, \quad \tilde{b}'_R = B\,\tilde{b}_R \tag{12}$$

Now all the three kinds of the SED basis functions are represented by the same non-uniform rectangular pulse functions with corresponding translations. Then the process of calculating the mutual-impedance elements between the SED basis functions can be further accelerated in the following way. The mutual-impedance element Z'_{m_0,m_0+m} between the m_0th SED basis function and the m_0+mth SED basis function can be obtained as follows.

$$Z'_{m_0,m_0+m} = \tilde{b}'^{T}_{l_{m_0}} C_m \tilde{a}'_{l_{m_0+m}} + \tilde{b}'^{T}_{l_{m_0}} D_m \tilde{b}'_{l_{m_0+m}} \tag{13}$$

where l_{m_0} and l_{m_0+m} could be 'L', 'R' or 'M', and depend on m_0 and m_0+m respectively. The size of C_m is $N^V \times N^U$, and the size of D_m is $N^V \times N^V$. The elements of the matrices C_m and D_m are $\langle U^V_{m_0,n_1}, L_1(U^U_{m_0+m,n_2})\rangle$ and $\langle U^V_{m_0,n_1}, L_2(U^V_{m_0+m,n_2})\rangle$ respectively. As all the three kinds of the SED basis functions are represented by the same non-uniform rectangular pulse functions with corresponding translations, the matrices C_m and D_m only depend on m, but they are independent of m_0. For a grating with M elements, $M(M-1)$ mutual-impedance elements in (7) need to be calculated. Through the above way and considering the symmetry of the Green's function, only $(M-1)\,N^V\left(2N^U+N^V\right)$ inner product operations are needed for filling the off-diagonal part of the impedance matrix of the SED basis functions.

3. NUMERICAL RESULTS

The method in this paper and the classical full-domain FDFD method are used to analyze dielectric gratings respectively in order to compare their efficiencies. In both the two examples, the same element (see Figure 2) is adopted, and the number of elements is 60. In the first

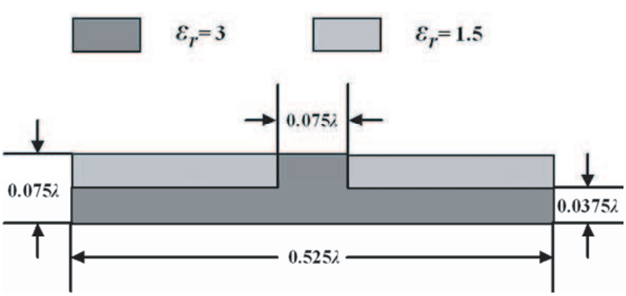

Figure 2. The geometry of an element is shown above.

Table 1. Normalized computational time.

	Example 1	Example 2
The classical full-domain FDFD method	100%	100%
The method in this paper	36%	18%

example the space l (see Figure 1) between the elements is 0.3λ, and in the second example the space l is 0.625λ. Both the two gratings are illuminated by TE wave at the incident angle (θ) of $45°$. For both the two methods, the side length of Yee's cells is 0.0125λ. For the classical full-domain FDFD method, perfect match layer (PML) is used to truncate the computational domain and the number of layers is 12. The Yee's cells of the classical full-domain FDFD method in the two examples are 46×4000 and 46×5560 respectively. For the method in this paper, the maximum wavelet decomposition level is 2, and the threshold valve is 0.05. Both the two methods are programmed with Matlab 7.0 and running in a desktop computer (CPU: P4 3.2 GHz). From Figure 3 and Table 1, it can be seen that in both the

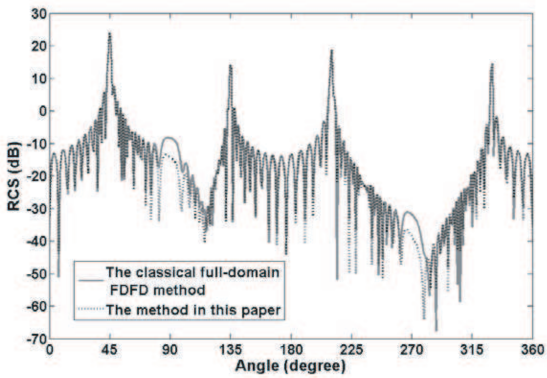

(a) The space l between the elements is 0.3λ

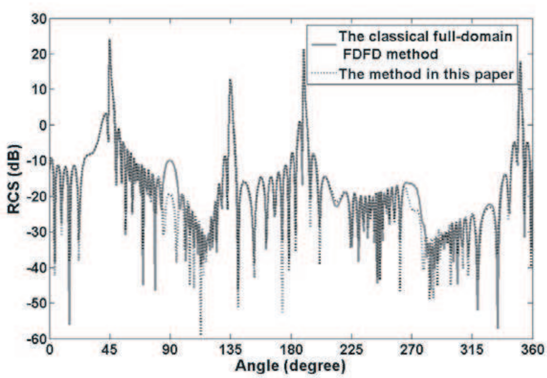

(b) The space l between the elements is 0.625λ

Figure 3. The RCSs obtained by the classical full-domain FDFD method and the method in this letter respectively.

two examples, the RCSs obtained by the two methods respectively are consistent, but the total computational times are largely reduced in the method presented in this paper, and this is more evident as the space l between the elements becomes large.

4. CONCLUSION

In this paper, the FDFD method, IE method and SED basis functions are combined to analyze scatterings from finite periodic dielectric gratings. The classical FDFD equations and a boundary integral equation are set up inside sub-domains and on the boundaries of sub-domains respectively, and the SED basis functions are applied on the boundary of the whole grating. Through the wavelet method, the expressions of the SED basis functions expanded by uniform rectangular pulse functions are modified to be expanded by non-uniform rectangular pulse functions with difference sizes, in order to reduce the number of inner product operations in calculating the mutual-impedance elements between the SED basis functions. In the numerical examples, the RCS curves obtained by the method in this paper are in good agreement with those obtained by the classical full-domain FDFD method, but the computational times are largely reduced in the former. The additional advantage of the method in this paper is that unlike the classical full-domain FDFD method there is no need to store and solve large matrix problems in it. Extracting the SED basis functions with more sub-domains may be a way to improve the accuracy of the method, and the investigation of this is our further work.

ACKNOWLEDGMENT

This work was supported by the Doctoral Program of Higher Education of China (No. 20060614005).

REFERENCES

1. Rappaport, C. M. and B. J. McCartin, "FDFD analysis of electromagnetic scattering in anisotropic media using unconstrained triangular meshes," *IEEE Trans. Antennas Propag.*, Vol. 39, No. 3, 345–349, March 1991.
2. Zhao, W., H. W. Deng, and Y. J. Zhao, "Application of 4-component compact 2-D FDFD method in analysis of lossy circular metal waveguide," *Journal of Electromagnetic Waves and Applications*, Vol. 22, No. 17–18, 2297–2308, December 2008.

3. Song, J. M. and W. C. Chew, "Multilevel fast-multipole algorithm for solving combined field integral equations of electromagnetic scattering," *Microwave Opt. Tech. Lett.*, Vol. 10, No. 1, 14–19, September 1995.
4. Khalaj-Amirhosseini, M., "Analysis of longitudinally inhomogeneous waveguides using the method of moments," *Progress In Electromagnetics Research*, PIER 74, 57–67, 2007.
5. Norgren, M., "A hybrid FDFD-BIE approach to two-dimensional scattering from an inhomogeneous biisotropic cylinder," *Progress In Electromagnetics Research*, PIER 38, 1–27, 2002.
6. Cui, T. J., W.-B. Lu, Z.-G. Qian, X. X. Yin, and W. Hong, "Sub-entire-domain basis function method for large-scale periodic structures," *Proc. IEEE Int. Symp. Antennas Propag.*, Vol. 4, 4459–4462, June 2004.
7. Lu, W. B., T. J. Cui, Z. G. Qian, X. X. Yin, and W. Hong, "Accurate analysis of large-scale periodic structures using an efficient sub-entire-domain basis function method," *IEEE Trans. Antennas Propag.*, Vol. 52, No. 11, 3078–3085, November 2004.
8. Du, P., B.-Z. Wang, H. Li, and G. Zheng, "Scattering analysis of large-scale periodic structures using the sub-entire domain basis function method and characteristic function method," *Journal of Electromagnetic Waves and Applications*, Vol. 21, No. 14, 2085–2094, December 2007.
9. Lu, W. B., Q. Y. Zhao, and T. J. Cui, "Sub-entire-domain basis function method for irrectangular periodic structures," *Progress In Electromagnetics Research B*, Vol. 5, 91–105, 2008.
10. Du, P., B.-Z. Wang, and J. Deng, "An extended simplified sub-entire domain basis function method for finite-sized periodic structures," *Journal of Electromagnetic Waves and Applications*, Vol. 22, No. 11–12, 1479–1488, October 2008.
11. Taflove, A. and S. C. Hagness, *Computational Electrodynamics: The Finite-difference Time-domain Method*, Artech House, New York, 2000.
12. Wang, B.-Z., R. Mittra, and W. Shao, "A domain decomposition finite-difference method utilizing characteristic basis functions for solving electrostatic problems," *IEEE Trans. Electromagn. Compat.*, Vol. 50, No. 4, 946–952, November 2008.
13. Murphy, W. D., V. Rokhlin, and M. S. Vassiliou, "Solving electromagnetic scattering problems at resonance frequencies," *J. Appl. Phys.*, Vol. 67, No. 10, 6061–6065, May 1990.